Fast and highly anisotropic thermal transport through vertically aligned carbon nanotube arrays

Ilia Ivanov,[a),b)] Alexander Puretzky, Gyula Eres, Hsin Wang, Zhengwei Pan, Hongtao Cui, Rongying Jin, Jane Howe, and David B. Geohegan[a),c)]
Oak Ridge National Laboratory, Oak Ridge, Tennessee 37831-6087

(Received 5 July 2006; accepted 17 October 2006; published online 28 November 2006)

This letter reports on fast and highly anisotropic thermal transport through millimeter-tall, vertically aligned carbon nanotube arrays (VANTAs) synthesized by chemical vapor deposition on Si substrates. Thermal diffusivity measurements were performed for both longitudinal and transverse to the nanotube alignment direction, with longitudinal values as large as 2.1 ± 0.2 cm^2/s and anisotropy ratios as large as 72. Longitudinal thermal conductivities of 15.3 ± 1.8 W/(m K) for porous 8 ± 1 vol % VANTAs in air and 5.5 ± 0.7 W/(m K) for epoxy-infiltrated VANTAs already exceed those of phase-changing thermal interface materials used in microelectronics. Data suggest that further improvements are possible through optimization of density and defects in the arrays. © *2006 American Institute of Physics*. [DOI: 10.1063/1.2397008]

Individual carbon nanotubes are predicted to have longitudinal thermal conductivities approaching 6000 W/(m K), and measured values of 3000 W/(m K) have been experimentally verified.[1,2] Such exceptionally high thermal conductivities originate from the large mean free path for phonons within the atomically perfect sp^2 carbon networks of idealized nanotubes.[3]

The ultimate realistic three-dimensional assembly of carbon nanotubes resulting in high thermal conductivity and anisotropy consists of (1) long, continuous nanotubes [Fig. 1(a)] to minimize the thermal resistance at nanotube junctions [Fig. 1(b)], (2) high packing density with minimized bundling, and (3) with few defects and high graphitic order for long-range phonon transport. However, attempts to date to assemble short nanotubes into macroscopic fibers,[4] papers,[5,6] or nanotube composites[7–9] have proved inadequate to address these requirements, resulting in thermal properties much lower than that of individual carbon nanotubes. The poor performance of macroscopic nanotube assemblies has been explained in terms of increased phonon scattering at nanotube junctions, inside the bundles, and at the nanotube sidewall defects.

Aligned forests of single-walled carbon nanotubes (SWNTs) have recently emerged as attractive candidates for thermal management, where the problem of phonon scattering at nanotube junctions might be solved.[10,11] While reproducible methods to grow long, pure SWNT arrays are still under development, the fabrication of millimeter-long vertically aligned carbon nanotube arrays (VANTAs) containing mixtures of SWNTs and few-walled multiwalled carbon nanotubes (MWNTs) has been achieved through the optimization of chemical vapor deposition (CVD) growth techniques utilizing *in situ* diagnostics, improved catalysts, and growth modeling.[12,13]

Here, longitudinal and transverse thermal diffusivities are reported for four samples of millimeter-tall VANTAs illustrated in Figs. 1(c) and 1(d), which were grown by two slightly different CVD techniques.[12,13] Details of the experimental setup, catalyst preparation and CVD growth have been described previously.[12,13] All VANTAs were grown by acetylene CVD on multilayer metal catalyst films consisting of 10 nm Al, 1 nm Fe, and 0.2 nm Mo deposited by e-beam evaporation on Si wafers at room temperature. However the 6-mm-tall samples VANTA2–VANTA4 were grown with the addition of ferrocene,[13] while the 2-mm-tall VANTA1 was grown without ferrocene.[12] The flash diffusivity method developed by Parker *et al.*[14] was used to measure the thermal diffusivities of the samples. VANTAs were detached from the silicon wafer with a razor blade and mounted by taping the sides of the array to the front side of a metal iris diaphragm, which was positioned at 8 mm from the window of a 2×2 mm^2 liquid nitrogen cooled InSb detector. The VANTA sample was separated from the metal diaphragm by a 2-mm-thick ring of modeling clay (Pasticolor, Ormya). The

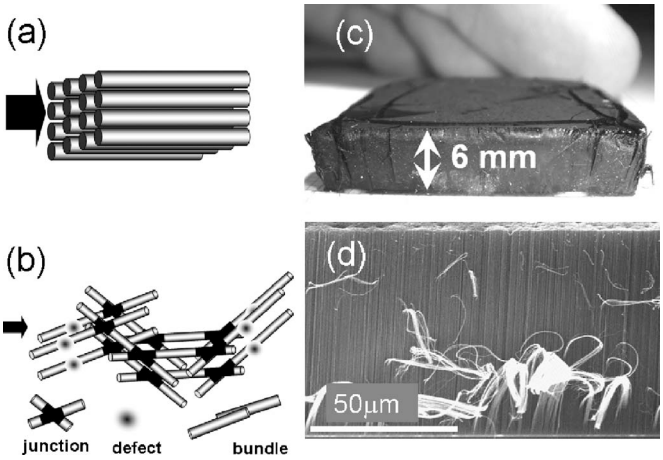

FIG. 1. (a) Schematic of the idealized structure for highly anisotropic and efficient heat transport. Perfectly aligned, continuous nanotubes packed in high density completely eliminate the high thermal resistance at nanotube junctions. (b) Schematic drawing of loose nanotube networks as found in bucky paper or chemically spun fibers comprised of short nanotubes. Thermal transport through the network in the direction of the arrow is limited by nanotube bundling, the presence of sidewall defects, and a large number of high thermal resistance nanotube junctions. (c) Photograph of 6-mm-tall VANTA. (d) Scanning electron micrograph of the top 70 μm of VANTA.

[a)]Authors to whom correspondence should be addressed.
[b)]Electronic mail: ivanovin@ornl.gov
[c)]Electronic mail: geohegandb@ornl.gov

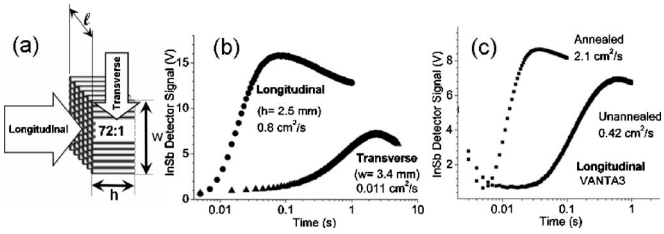

FIG. 2. (a) Schematics showing the orientation of nanotubes in VANTAs for anisotropy of thermal diffusivity measurements. Thermal diffusivity is calculated from the half rise time of the signal. The anisotropy of thermal diffusivity is defined by the ratio of the longitudinal (0.8 ± 0.2 cm^2/s) to transverse (0.011 ± 0.001 cm^2/s) diffusivities, and equals 72 for this sample, (VANTA2). (b) Detector response on the backside of the carbon nanotube arrays oriented longitudinally ($h=2.5$ mm) and transversely ($w=3.4$ mm) to the direction of the heat pulse induced. (c) Faster rise time of the detector response for annealed VANTA3, which corresponds to the improved thermal diffusivity of 2.1 ± 0.2 cm^2/s compared to that of 0.42 ± 0.06 cm^2/s for unannealed carbon nanotubes.

sample was excited by an 8 ms pulse from a 2.4 kW Xe lamp (Acute 2-2400, Profoto) positioned 300 mm from the VANTA sample. The details of the experimental thermal diffusivity setup, LabVIEW based interface, and data fitting procedures were described elsewhere.[15]

In all measurements the sample was at least 2 mm thick, and the aperture of the iris diaphragm was 2 mm or smaller. For the longitudinal measurements the width, the length, and the height of the VANTA samples were 10–20, 10–20, and ~2 mm, respectively, and a 2 mm aperture was used. For the transverse measurements these dimensions were ~2, 10, and 10 mm, respectively. The VANTA3 and VANTA4 samples were cleaved into two pieces and detached from their Si substrates, and a piece from each sample was annealed in Ar at 2800 °C for 2 h. A 2-mm-thick sample of bulk SiC with known thermal diffusivity of 0.0354 cm^2/s was used as a calibration standard.

The longitudinal thermal diffusivities of different VANTAs measured at room temperature in air varied between 0.42 ± 0.06 and 0.9 ± 0.1 cm^2/s. The highest thermal diffusivity for VANTA1 of $0.9+0.1$ cm^2/s is comparable to that of pure aluminum, 0.96 cm^2/s.[16] Transverse thermal diffusivities as illustrated in Fig. 2(a) could be only measured for arrays taller than 2 mm in height (VANTA2–VANTA4). Figure 2(b) shows two detector traces for VANTA2, corresponding to measurements in longitudinal and transverse orientations of the array. The thermal anisotropy is given by the ratio of longitudinal to transverse thermal diffusivities. The highest measured thermal anisotropy of 72 is a factor of 3 smaller than that of highly ordered pyrolytic graphite,[17] but a factor of 7 larger than that reported for magnetically aligned SWNT bucky paper.[5,6]

Defects in the carbon network perturb the conjugation of the perfect π system of the nanotubes, degrading their thermal conductivity by providing scattering sites for phonons.[18] High resolution transmission electron microscopy (HRTEM) was used to explore the presence of defects in the carbon nanotubes. In addition to the sidewall defects shown in Fig. 3(b), the number of walls and the diameter of some nanotubes were observed to change. However, the nature and density of these defects (e.g., Stone-Wales defects, carbonyl, carboxyl, and hydroxyl groups) could not be quantified from the HRTEM images.

The ratio of the Raman tangential G-band intensity to the disorder-induced D band is often used to compare the graphitic ordering in carbon materials.[19] The increase in the G to D band ratio has been shown to correlate with higher crystallinity and higher thermal conductivity for carbon fibers.[20] The G/D band intensity ratios were measured at more than ten locations along the length of each cross-sectioned VANTA. For VANTA2–VANTA4 constant G/D ratios of less than 1 were observed and no evidence of the radial breathing modes (RBM) characteristic of SWNTs was found. Sample VANTA1 included some SWNTs as evidenced by the RBM in the Raman spectra, and the G/D ratio increased from 1 to 4 measured from the base toward the top of the array.

The VANTA samples with the lowest thermal diffusivity (VANTA3 and VANTA4) were annealed in argon at 2800 °C for 2 h (Ref. 20) to improve the nanotube crystallinity and gauge the resulting effect on thermal diffusivity. Figure 3(a) shows that after annealing, the Raman G/D band ratios for both samples increased by a factor of 8. The RBM region of the Raman spectrum in the inset of Fig. 3(a) showed no change after annealing, eliminating formation of SWCNT as a possible cause for the observed G/D ratio increase. HRTEM images of nanotubes after annealing in Fig. 3(c) show cleaner sidewalls, fewer sidewall defects and healing of discontinuities at the junctions between nanotube segments with different diameters. We interpret these changes to be responsible for the increase in G/D band ratio. The thermal diffusivity of annealed VANTAs increased in a range from three to five times. Figure 2(c) shows two detector traces (before and after 2800 °C annealing) for sample VANTA3 mounted with the nanotubes oriented longitudinally. Annealing results in a faster rise time of the signal, indicating improved ther-

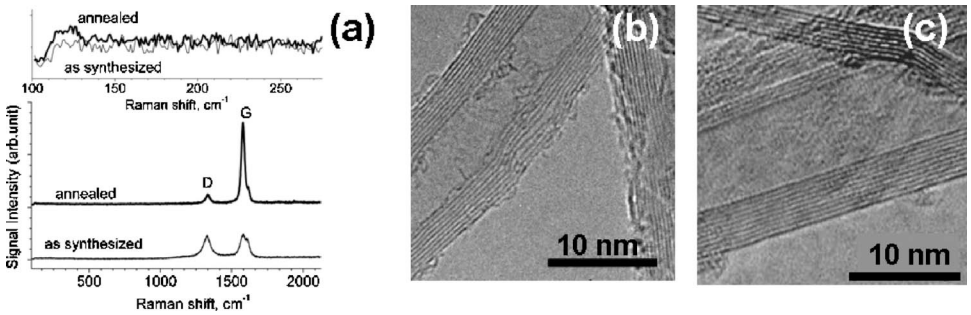

FIG. 3. (a) Raman spectra of VANTA4 before and after annealing at 2800 °C were measured with the polarization of the 632.8 nm HeNe laser parallel to the orientation of the carbon nanotubes. The ratio of G/D band intensities in the Raman spectrum increases by a factor of 8 as a result of annealing. The inset demonstrates no changes in the RBM region of the Raman spectrum after annealing. (b) HRTEM image of carbon nanotubes in VANTA4 before annealing with sidewall defects. (c) HRTEM image of carbon nanotubes in VANTA4 after annealed showed reduced numbers of sidewall defects.

mal diffusivity from 0.42 ± 0.06 to 2.1 ± 0.2 cm^2/s for sample VANTA3. The same annealing procedure resulted in a thermal diffusivity increase from 0.42 ± 0.06 to 1.4 ± 0.1 cm^2/s for sample VANTA4. These results confirm that the crystallinity of the nanotubes, in addition to their continuity and spacing, is an important factor that affects the thermal properties of the arrays.

The thermal conductivity of VANTA in air k_{VA} was estimated as $k_{VA}=\alpha_{VA}\rho_{VA}c_p$, where α_{VA} is the measured thermal diffusivity, and ρ_{VA} and c_p are the average density and the specific heat capacity of VANTAs and air, respectively. The averaged density and the specific heat capacity were calculated as the sum of the volume ($\delta_{V,VANTA}=0.08$) and mass ($\delta_{m,VANTA}=0.99$) fractional densities and the specific heat capacities of these two components, respectively, using $\rho_{VANTA}=1900\pm100$ kg/m^3, $\rho_{air}=1.2$ kg/m^3, $c_{p,VANTA}=470$ $J/(kg\,K)$, and $c_{p,air}=1.0$ $kJ/(kg\,K)$. The longitudinal thermal conductivities for as synthesized arrays in air were found to be 6.4 ± 0.8, 5.7 ± 0.7, 3.0 ± 0.4, and 3.0 ± 0.4 $W/(m\,K)$ for VANTA1–VANTA4, respectively. The corresponding transverse thermal conductivities were found to be 0.08 ± 0.01, 0.14 ± 0.02, and 0.14 ± 0.02 $W/(m\,K)$ for VANTA2–VANTA4 respectively. The thermal conductivity increases to 15 ± 2 and 10 ± 1 $W/(m\,K)$ for longitudinal direction in the annealed VANTA 3 and VANTA4, respectively. Despite the high porosity of the arrays, the highest thermal conductivity of VANTAs in air is a factor of 3 higher than that of currently used phase-changing thermal interface materials (PCMs), which consist of a polymer (polyolefins, epoxies, polyesters, and acrylics) mixed with thermally conductive fillers.[21]

Infiltration of VANTAs with epoxy was enabled by the porosity of the arrays. VANTAs were vacuum impregnated with epoxy resin (SpeciFix-40, Struers) and cured for 4 h at 60 °C in a dry box prior to thermal diffusivity measurements. For an epoxy-infiltrated VANTA (8 ± 1 vol %, unannealed, 2-mm-long MWCNT, and Raman G/D band ratio of 3) the same approach was used as described for the VANTA-air composite to estimate [using instead $\rho_{epoxy}=1090$ kg/m^3 and $c_{p,epoxy}=1890$ $J/(kg\,K)$] a thermal conductivity of 5.5 ± 0.7 $W/(m\,K)$. This corresponds to a factor of 20 improvement compared to the thermal conductivity of pure epoxy and a factor of 6.3 improvement compared to previously reported thermal conductivity of VANTA silicon elastomer 706 composite.[22]

In conclusion, we report that VANTAs exhibit higher thermal diffusivity and anisotropy than any other macroscopic nanotube assembly to date. VANTAs are conceptually similar to the idealized structure of material for optimal anisotropic heat transport in Fig. 1(a). Further improvement in the thermal properties of VANTAs is possible through optimization of the growth conditions for arrays which are more crystalline, straight, and dense. The thermal diffusivity of these porous arrays already exceeds that of aluminum and copper, and thermal conductivities reported here for annealed arrays are triple that for comparable PCM. Combined with the resilient mechanical performance recently measured for VANTAs,[23] these conformable and springy nanotube assemblies offer unique multifunctional materials for thermal management and sensing applications.

Synthesis science [I.I., A.P., G.E., D.G., R.J., H.C., Z.P.] supported by DOE Office of Basic Energy Sciences, Division of Materials Science and Engineering. [J.H., H.W.] supported by DOE Office of Transportation Technologies, Energy Efficiency and Renerable Energy. The authors also acknowledge helpful discussions with Ralph Dinwiddle, Art Miller, and Roland Seals and equipment development funded by DARPA's Defense Science Office. Oak Ridge National Laboratory is managed and operated by UT-Battelle, LLC for the U.S. Department of Energy under contract DE-AC05-00OR22725.

[1] S. Berber, Y. Kwon, and D. Tomanek, Phys. Rev. Lett. **84**, 4613 (2000).
[2] P. Kim, L. Shi, A. Majumdar, and P. L. McEuen, Phys. Rev. Lett. **87**, 215502 (2001).
[3] J. Hone, B. Batlogg, Z. Benes, A. T. Johnson, and J. E. Fischer, Science **289**, 1730 (2000).
[4] W. Zhou, J. Vavro, C. Guthy, K. I. Winey, J. E. Fischer, L. M. Ericson, S. Ramesh, R. Saini, V. A. Davis, C. Kittrell, M. Pasquali, R. H. Hauge, and R. E. Smalley, J. Appl. Phys. **95**, 649 (2004).
[5] J. E. Fischer, W. Zhou, J. Vavro, M. C. Llaguno, C. Guthy, R. Haggenmueller, M. J. Casavant, D. E. Walters, and R. E. Smalley, J. Appl. Phys. **93**, 2157 (2003).
[6] J. Hone, M. C. Llaguno, N. M. Nemes, A. T. Johnson, J. E. Fischer, D. A. Walters, M. J. Casavant, J. Schmidt, and R. E. Smalley, Appl. Phys. Lett. **77**, 666 (2000).
[7] R. S. Ruoff and D. C. Lorents, Carbon **33**, 925 (1995).
[8] C. H. Liu, H. Huang, Y. Wu, and S. S. Fan, Appl. Phys. Lett. **84**, 4248 (2004).
[9] G. D. Zhan, J. D. Kuntz, H. Wang, C. M. Wang, and A. K. Mukherjee, Philos. Mag. Lett. **84**, 419 (2004).
[10] K. Hata, D. N. Futaba, K. Mizuno, T. Namai, M. Yumura, and S. Iijima, Science **306**, 1362 (2004).
[11] Y. Miyauchi, S. Chiashi, Y. Murakami, Y. Hayashida, and S. Maruyama, Chem. Phys. Lett. **387**, 198 (2004).
[12] A. A. Puretzky, D. B. Geohegan, S. Jesse, I. N. Ivanov, and G. Eres, Appl. Phys. A: Mater. Sci. Process. **63**, 1851 (2005).
[13] G. Eres, A. A. Puretzky, D. B. Geohegan, and H. Cui, Appl. Phys. Lett. **84**, 1759 (2004).
[14] W. J. Parker, R. J. Jenkins, C. P. Butler, and G. L. Abbott, J. Appl. Phys. **32**, 1679 (1961).
[15] H. Wang and R. B. Dinwiddie, *Development of a LabView Based Portable Thermal Diffusivity System* (DEStech, Knoxville, TN, 2004), Vol. 27, p. 484.
[16] J. E. Jensen, R. B. Stewart, W. A. Tuttle, and A. G. Prodell, *Brookhaven National Laboratory Selected Cryogenic Data Notebook*, BNL 10200-R (Brookhaven National Laboratory, New York, 1980), Vol. 1, p. XV-A-1.
[17] H. Kato, T. Baba, and O. Masahiro, Meas. Sci. Technol. **12**, 2074 (2001).
[18] C. Jianwei, T. Cagin, and W. A. I. Goddard, Nanotechnology **11**, 68 (2000).
[19] A. C. Ferrari and J. Robertson, Phys. Rev. B **61**, 14095 (2000).
[20] J. Heremans, I. Rahim, and M. S. Dresselhaus, Phys. Rev. B **32**, 6742 (1985).
[21] E. C. Samson, S. V. Machiroutu, J. Y. Chang, I. Santos, J. Hermerding, A. Dani, R. Prasher, and D. W. Song, Intel Technol. J. **09**, 87 (2005).
[22] H. Huang, C. Liu, Y. Wu, and S. Fan, Adv. Mat. **17**, 1652 (2005).
[23] A. Cao, P. L. Dickrell, W. G. Sawyer, M. N. Ghasemi-Nejhad, and P. Ajayan, Science **310**, 1307 (2005).